

TrAISformer—A generative transformer for AIS trajectory prediction

Duong Nguyen, *Member, IEEE*, and Ronan Fablet, *Senior Member, IEEE*

Abstract—Predicting the position of a vessel at a specific time in the future is at the core of many maritime applications. The Automatic Identification System (AIS) provides rich information to enable this task. However, vessel trajectory forecasting using AIS data is challenging, even for modern machine learning/deep learning models, because motion data in general, and AIS data in particular, are complex and multimodal. In this paper, we tackle those difficulties by introducing a novel discrete, high-dimensional representation of AIS data and a new loss function to explicitly account for heterogeneity and multimodality. The proposed model—referred to as *TrAISformer*—is a modified transformer network that extracts long-term correlations of AIS trajectories in the proposed enriched space to forecast the positions of vessels after several hours. We report experimental results on real, public AIS data. *TrAISformer* significantly outperforms state-of-the-art methods and reaches a mean prediction performance below 10 nautical miles up to ~ 10 hours.

Index Terms—AIS, vessel trajectory, trajectory prediction, maritime surveillance, multimodal data, deep learning, transformer.

I. INTRODUCTION

With the continuous growth of maritime traffic, maritime surveillance (MS) and Maritime Situational Awareness (MSA) involve critical issues, among which vessel trajectory prediction is a key challenge. Knowing where vessels are heading to and their approximate positions at a specific time in the future, especially from a few hours ahead to tens of hours ahead, is extremely useful in many applications, such as search and rescue [1], [2], traffic control [3], path planning [4], port congestion avoidance [5]–[7], pollution monitoring [8].

The Automatic Identification System—AIS provides invaluable data for the monitoring and surveillance of maritime traffic. AIS data provide vessels' kinetic information (the current position indicated by the latitude and longitude coordinates, the current Speed Over Ground—SOG, the current Course Over Ground—COG, *etc.*), the information of the voyages, as well as the static information (the identification number in the format a Maritime Mobile Service Identity—MMSI number, the name of the vessel, *etc.*) of vessels in the vicinity. Vessel trajectory prediction using AIS data has been studied for more than a decade [9]–[16]. However, the achievements

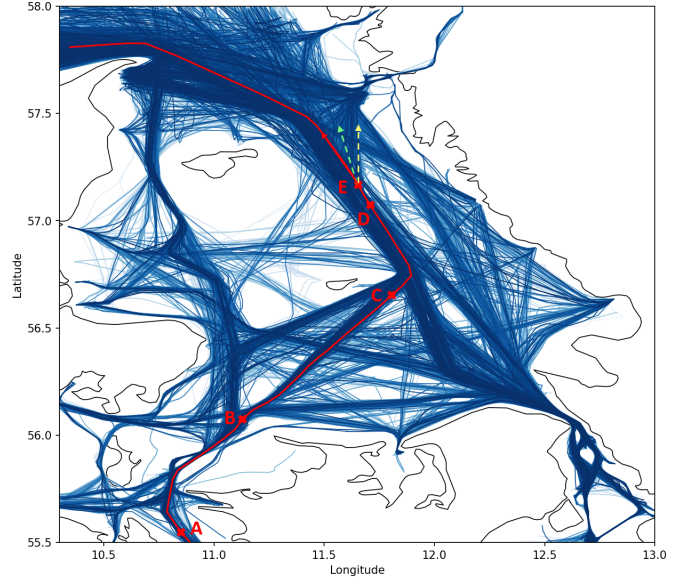


Fig. 1: Illustration of long-term dependence patterns in AIS trajectories: At **E**, vessels would normally follow one of the two main maritime routes indicated by the red and the yellow dashed arrows. In order to forecast whether a vessel continues straight ahead (red) or turns right (yellow), the prediction model may need to roll back several time steps to **D**, **C**, **B**, and **A** to know where this vessel comes from. Furthermore, if the model is not multimodal, it may output as a prediction the unusual green dashed path, as a merger of the true red and yellow paths.

are still limited. Most state-of-the-art schemes reach relevance prediction performance only for short time horizons (from a few minutes to half an hour) [12], [17], or for longer time-horizons under very specific movement patterns corresponding to predefined maritime routes [18], [19] or unimodal movement patterns [16], [17]. Due to the complexity of vessel movement patterns and the heterogeneous nature of AIS data, forecasting vessel positions above several hours remain highly challenging. As an illustration, we report in Fig. 1 two vessel paths with very similar movement patterns on segment **C**→**D** but heading to two different destinations.

Trajectory prediction issues have received a growing attention, with a focus on pedestrian and vehicle movement patterns [20], [21]. Deep learning schemes have become the state-of-the-art approaches [22]–[26]. These recent advances however barely transfer to AIS trajectory prediction. First, the targeted space-time scales strongly differ (e.g., meters and a

Duong Nguyen and Ronan Fablet are with IMT Atlantique, Lab-STICC, 29238 Brest, France (email: nvduong0512@gmail.com and ronan.fablet@imt-atlantique.fr)

This work was supported by public funds (Ministère de l'Éducation Nationale, de l'Enseignement Supérieur et de la Recherche, FEDER, Région Bretagne, Conseil Général du Finistère, Brest Métropole). It benefited from HPC and GPU resources from Azure (Microsoft EU Ocean awards) and from GENCI-IDRIS (Grant 2020-101030). The authors also acknowledge the support of ANR (French Agence Nationale de la Recherche) under reference ANR AI Chair OceaniX (ANR-19-CHIA-0016).

few seconds to a few minutes for pedestrian movements vs. kilometers and hours for vessel movements). Second, while interaction issues are critical to understand and predict pedestrian and vehicle trajectories, such interactions have negligible effects in vessels' movements in the open sea. Third, long-term dependencies are key factors for the latter.

In the open sea, vessels often follow some common movement patterns due to traffic regulation constraints and fuel consumption optimization [27], [28]. However, the analysis of the maritime traffic according to a finite set of interconnected maritime routes using clustering-based approaches [16]–[19] appears too simplistic to account for the heterogeneous and multimodal characteristics of AIS data exhibited by real-world datasets. The crux of vessel trajectory prediction for the targeted time horizon lies in the prediction of the turning direction at the “intersections” (called the *waypoints*) of maritime routes (see Fig. 1). This task may require the model to roll back many time steps to know where the vessel comes from and to fully understand large-scale movement patterns. Overall, we may distinguish the following two main methodological issues: i) learning how to represent maritime traffic flows beyond a fully-structured network of maritime routes; and ii) accounting for long-term patterns in vessels' trajectories.

To address these challenges, we propose a novel deep learning model, referred to as *TrAISformer*. Our key contributions are as follows:

- *TrAISformer* exploits a specific representation of AIS data and frames the prediction task as a classification problem to explicitly account for the heterogeneity of AIS data and the multimodality of vessel trajectories.
- We leverage a probabilistic transformer architecture to capture long-term dependencies in AIS trajectories.
- We benchmark *TrAISformer* w.r.t. state-of-the-art schemes on a real AIS dataset and report a prediction error below 10 nmi (nautical mile) up to 10 hours, which significantly outperforms previous works.

The paper is organized as follows. Section II states the problem and gives an overview of the related work and current limitations for AIS trajectory prediction. We present the proposed approach in Section III. Section IV details our numerical experiments. We further discuss our main contributions and future work in Section V.

II. PROBLEM STATEMENT AND RELATED WORK

AIS trajectory prediction comes to predict the future positions of vessels over a given time horizon, given a series of AIS data. Formally, let us denote by \mathbf{x}_t an AIS observation at time step t , where \mathbf{x}_t comprises the position of the vessel (indicated by the latitude and the longitude), its speed over ground, and its course over ground¹. An AIS trajectory is then represented by a series of observations $\{\mathbf{x}_{t_0}, \mathbf{x}_{t_1}, \dots, \mathbf{x}_{t_T}\}$ where $t_i < t_j$ if $i < j$. One can use some simple interpolation method to get a series of $T + 1$ equally sampled observations $\mathbf{x}_{0:T} \triangleq \{\mathbf{x}_{t_0}, \mathbf{x}_{t_0+\Delta t}, \mathbf{x}_{t_0+2*\Delta t}, \dots, \mathbf{x}_{t_0+T*\Delta t}\}$. The time step

Δt is chosen such that the effect on the downstream tasks of the error inherited from the interpolation is negligible. In this paper, we fix the time step at 10 minutes and omit Δt for the sake of notation simplicity, *i.e.* $\mathbf{x}_{t_0+n*\Delta t} \triangleq \mathbf{x}_{t_0+n}$.

The L -step-ahead prediction problem comes to predict the trajectory $\mathbf{x}_{T+1:T+L} = \{\mathbf{x}_{T+1}, \mathbf{x}_{T+2}, \dots, \mathbf{x}_{T+L}\}$ given the $T + 1$ observations $\mathbf{x}_{0:T} = \{\mathbf{x}_0, \mathbf{x}_1, \dots, \mathbf{x}_T\}$ up to time T . Given the nature of the prediction problem, it naturally arises as the sampling of the following conditional distribution:

$$p(\mathbf{x}_{T+1:T+L} | \mathbf{x}_{0:T}). \quad (1)$$

We may point out that this probabilistic formulation also embeds deterministic prediction models [12], [30], which reduces to Dirac distributions. Classically [12], [14], [16], [30], one considers a family of distribution that can be factorized as:

$$p(\mathbf{x}_{T+1:T+L} | \mathbf{x}_{0:T}) = \prod_{l=1}^L p(\mathbf{x}_{T+l} | \mathbf{x}_{0:T+l-1}). \quad (2)$$

This parameterization assumes a conditional independence of future states $\mathbf{x}_{T+1:T+L}$ w.r.t. past states $\mathbf{x}_{0:T+l-1}$. It generally offers a good grade-off between the modeling complexity and the representativeness of the model.

We may distinguish two main categories of approaches for AIS trajectory prediction. The first category relies on a state-space formulation. It combines a dynamical prior on the vessel movements and a filtering method, such as Kalman filter [31], [32] or particle filter [9], to infer or sample the posterior (1). Such schemes generally rely on simplistic dynamical priors such as the Curvilinear Motion Model (CMM) [31], which cannot account for complex patterns including turning points. The second category of approaches involves learning-based schemes. Recent works leverage deep learning methods, and specifically LSTM-based (Long Short-Term Memory) or GRU-based (Gated Recurrent Unit) models [33], [34], [35], to forecast AIS trajectories in a deterministic fashion. Given the multi-path patterns exhibited by AIS datasets, such schemes are likely to fail [36]. Clustering-based approaches [10], [12], [16], [17], [37] form another group of learning-based schemes. They assume that one can represent the maritime traffic over a given area as a graph, where each node refers to a waypoint and each edge refers to the maritime route between the corresponding two nodes. The prediction problem then resorts to exploit a forecasting model over the defined graph. A rich literature exists exploiting among others constant velocity model and particle filter [10], Gaussian Processes [11] and neural networks [16], [17]. However, all those schemes suffer from the limitation of the route-based representation of the maritime traffic, which applies to highly-structured maritime traffic only. Yet, in general, a significant fraction of AIS trajectories cannot be assigned to predefined routes [36], [38]. This explains why the application of clustering-based techniques in operational systems remain limited.

In this paper, we propose a novel model for AIS trajectory prediction, referred to as *TrAISformer*. To deal with the complex and multimodal nature of AIS trajectories, we use a new representation of AIS data and leverage the modeling power of deep learning, specifically of transformer architectures

¹We let the reader refer to [29] for a more detailed presentation of AIS data streams.

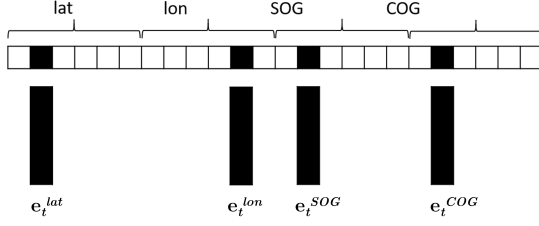


Fig. 2: **Proposed representation of AIS data:** For each attribute $att \in \{lat, lon, SOG, COG\}$, the observed value (which is continuous) is discretized into an one-hot vector \mathbf{h}_t^{att} . Each \mathbf{h}_t^{att} is then associated with a high dimensional real-valued embedding vector \mathbf{e}_t^{att} .

[39]. Contrary to clustering-based approaches, *TrAISformer* applies to any trajectory in the case-study region without any constraints regarding an explicit graph of maritime routes. Besides, we re-frame the prediction as a classification-based learning problem to best forecast the positions of maritime vessels several hours ahead.

III. PROPOSED APPROACH

In this section we detail the proposed approach. We introduce a new representation of AIS data, derive a new loss function and provide a brief introduction of the transformer architecture used in *TrAISformer*.

A. Discrete and sparse representation of AIS data

One of the main challenges in trajectory prediction in general, and AIS trajectory prediction in particular, is the representation of the heterogeneous and multimodal nature of motion data, given relatively low-dimensional observations. In this subsection we introduce a new representation of AIS data to tackle the heterogeneity part. The multimodality part will be addressed in the next subsection with a classification-based training loss.

The prevalent way to represent an AIS message is to use a 4-dimensional real-valued vector composed of the position and the velocity of the vessel:

$$\mathbf{x}_t \triangleq [lat, lon, SOG, COG]^T. \quad (3)$$

However, as discussed in [36] and [38], it is difficult to encode complex vessel movement patterns in this feature space. A natural idea is to expand to a higher-dimensional space, *i.e.* instead of modeling $p(\mathbf{x}_{T+1:T+L}|\mathbf{x}_{0:T})$, we consider $p(\mathbf{e}_{T+1:T+L}|\mathbf{e}_{0:T})$, with $\mathbf{e}_t \in \mathbb{R}^{d_e}$ a high-dimensional embedding vector of \mathbf{x}_t . Recently, variational autoencoders have been very successful in learning such effective mappings that encode \mathbf{x}_t to \mathbf{e}_t , and decode \mathbf{e}_t back to \mathbf{x}_t [40]–[45]. However, when the dimension of \mathbf{e}_t is much higher than that of \mathbf{x}_t , the training becomes extremely difficult because of overfitting.

To overcome those overfitting problems, we inherit the idea of the “four-hot” vector \mathbf{h}_t in our previous works [36] and [38], where the latitude, the longitude, the SOG and the COG are discretized into N_{lat} , N_{lon} , N_{SOG} , and N_{COG} bins, respectively. Each attribute bin is then associated with a high dimensional embedding vector \mathbf{e}_t^{att} ($att \in \{lat, lon, SOG, COG\}$).

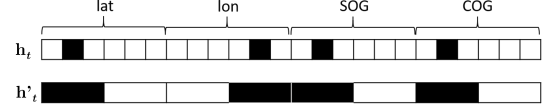


Fig. 3: **Example of multi-resolution “four-hot” vectors for AIS data:** The model uses the fine-resolution vector \mathbf{h}_t in the embedding module (see Fig.2), while the loss function uses both \mathbf{h}_t and a coarse-resolution \mathbf{h}'_k .

The embedding vector \mathbf{e}_t of an AIS observation \mathbf{x}_t is the concatenation of \mathbf{e}_t^{att} . This mapping is illustrated in Fig. 2. By doing so, we guarantee that in the embedding space, only $N_{lat} \times N_{lon} \times N_{SOG} \times N_{COG}$ values of \mathbf{e}_t will be used. This sparse constraint acts as a regularizer that allows us to augment the original 4-dimensional representation of AIS observation \mathbf{x}_t to a much higher dimensional space of \mathbf{e}_t without overfitting [46]. An AIS trajectory is then represented by a time series $\{\mathbf{e}_0, \mathbf{e}_1, \dots, \mathbf{e}_T\}$.

Note that from \mathbf{x}_t we can easily construct \mathbf{h}_t , and the mapping $\mathbf{h}_t \rightarrow \mathbf{e}_t$ is one-to-one. However, in the backward direction, from \mathbf{h}_t we can not find the exact \mathbf{x}_t because of the discretization. In this paper, we approximate \mathbf{x}_t by simply using the mid-points of the bins indicated by \mathbf{h}_t . The trade-off between the precision of \mathbf{x}_t and the efficiency of models using \mathbf{h}_t has been discussed in our previous works [36], [38].

B. Learning scheme

In the learning literature, trajectory prediction is often stated as a regression problem, such that a model outputs the best possible continuous-valued $\mathbf{e}_{T+1:T+L}$ (or $\mathbf{x}_{T+1:T+L}$) given the input $\mathbf{e}_{0:T}$ (or $\mathbf{x}_{0:T}$) [12], [16]. Within a deterministic setting, the most common loss function is the mean square error between the predicted values and the true values [12], [17], [47]:

$$\mathcal{L}_{MSE} \triangleq \sum_{l=1}^L \|\mathbf{x}_{T+l}^{pred} - \mathbf{x}_{T+l}^{true}\|_2^2, \quad (4)$$

where $\|\cdot\|_2$ denotes the Euclidean norm L_2 . However, while this L_2 loss function can be interpreted w.r.t. Gaussian assumption on the conditional likelihood $p(\mathbf{e}_{T+l}|\mathbf{e}_{0:T+l-1})$ (or $p(\mathbf{x}_{T+l}|\mathbf{x}_{0:T+l-1})$), it may not be appropriate for multimodal posterior distributions as illustrated by vessels’ trajectories in Fig.1. To explicitly account for multimodal posteriors, we introduce a classification-based formulation, which relies on modeling $p(\mathbf{e}_{T:T+L}|\mathbf{e}_{0:T+l-1})$ as a categorical distribution. Because the mapping $\mathbf{h}_t \rightarrow \mathbf{e}_t$ is one-to-one, we have:

$$p(\mathbf{h}_{T+l}|\mathbf{e}_{0:T+l-1}) = p(\mathbf{e}_{T+l}|\mathbf{e}_{0:T+l-1}). \quad (5)$$

As \mathbf{h}_t is a “four-hot” vector, this becomes a classification problem with four heads (each head is for one one-hot vector component of \mathbf{h}_t). Let us denote $p_{T+l} \triangleq p(\mathbf{h}_{T+l}|\mathbf{e}_{0:T+l-1}) = p(\mathbf{e}_{T+l}|\mathbf{e}_{0:T+l-1})$, the loss function is defined as:

$$\mathcal{L}_{CE} \triangleq \sum_{l=1}^L CE(p_{T+l}, \mathbf{h}_{T+l}), \quad (6)$$

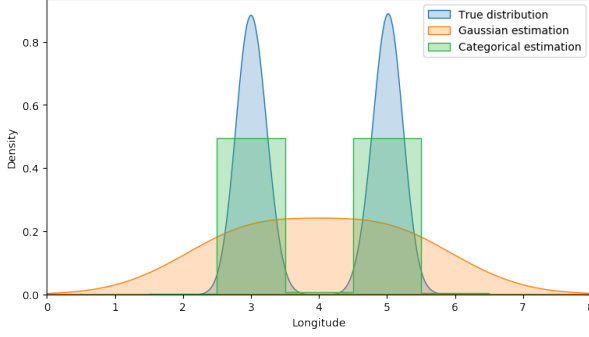


Fig. 4: **Illustration of loss function \mathcal{L}_{CE} to account for multimodal posterior:** Suppose that at a specific waypoint, half of the vessels in the training set turn left and the other half turn right. The true distribution of the longitude at the next time step is a bimodal normal distribution, depicted by the blue curve. If we use a real-valued scalar to represent the longitude and use \mathcal{L}_{MSE} as the loss function, the implicit distribution of the model is a unimodal Gaussian distribution. This model would merge the two modes of the true distribution, as shown by the orange curve. By contrast, if we use a one-hot vector to represent the longitude and the \mathcal{L}_{CE} as the loss function, the implicit distribution of the model is a Categorical distribution. With this distribution, the model preserves the two modes, as shown by the green curve.

with CE is the cross-entropy function. In Fig. 4 we explain how this loss function helps the model preserve the multimodal nature of the data.

Note that \mathbf{h}_t is a discrete representation of \mathbf{x}_t . This discretization can be performed at different resolutions. We empirically observed that the prediction could be slightly improved if we use a multi-resolution version of \mathcal{L}_{CE} (see Fig. 3) as follows:

$$\mathcal{L}_{CE} = \sum_{l=1}^L CE(p_{T+l}, \mathbf{h}_{T+l}) + \beta CE(p'_{T+l}, \mathbf{h}'_{T+l}). \quad (7)$$

with $p'_{T+l} \triangleq p(\mathbf{h}'_{T+l} | \mathbf{e}_{0:T+l-1})$, \mathbf{h}'_k is a coarser version of \mathbf{h}_t , β is a scalar controlling the weight of the coarse-resolution loss.

C. Transformer architecture

As illustrated in Fig. 1, in order to forecast the trajectory of a vessel correctly, a prediction model needs to capture possible long-term dependencies in the historical AIS observations. Transformer neural networks [39] naturally arise as relevant candidates in this context. Here, we use a transformer that is similar to GPT models [48]. The architecture is presented briefly in the next paragraphs. Interested readers are referred to [49] for a more complete and formal introduction of transformer.

The transformer network in our model stacks a series of attention layers. Each layer is an auto-regressive model that uses dot-product multiple-head self-attention mechanisms:

$$\text{Attention}(Q, K, V) = \text{softmax}\left(\frac{QK^T}{\sqrt{d_e}}\right) V, \quad (8)$$

with Q, K, V are linear projections of the input sequence $(\{\mathbf{e}_t\})$ for the first layer, or the output sequence of the previous layer for other layers). At each layer, the input sequence is projected to a new space V , the output of the attention block is a weighted sum in V , where the weights indicate the relative contribution of each time step. These weights are computed as $\text{softmax}(QK^T/\sqrt{d_e})$. The projection operators Q, K, V are learned during the training phase and the calculation is performed in parallel. By doing so, the model can directly retrieve information from several time steps in the past. This is a critical feature compared with recurrent networks, where the model have to process data sequentially and may not be able to retrieve long-term information.

The output of the final layer of the transformer is split into four parts corresponding to the four attributes (lat, lon, SOG, COG) of \mathbf{x}_t . As we formulate the prediction as a classification problem, each part is then fed into a softmax layer to compute p_{T+l} . p'_{T+l} is obtained by simply merging the bins of the prediction of \mathbf{h}_t .

We apply this model recursively. To forecast a vessel position at time $T + l$, we sample a “four-hot” vector \mathbf{h}_{T+l}^{pred} from p_{T+l} :

$$\mathbf{h}_{T+l}^{pred} \sim p(\mathbf{h}_{T+l} | \mathbf{e}_{0:T+l-1}) \quad (9)$$

and compute the “pseudo-inverse” of the sampled “four-hot” vector to output the new position \mathbf{x}_{T+l}^{pred} . The latter is then fed to the network to sample similarly a position at the next time step. We iterate this sampling procedure up to the desired trajectory length. We may also run this sampling procedure several times for a given AIS trajectory to generate different possible predicted paths. This stochastic procedure then allows us to address the fact that two vessels currently having similar movement patterns may go in different directions at the next waypoint. We demonstrate in Section IV that if we do not sample \mathbf{h}_{T+l}^{pred} from $p(\mathbf{h}_{T+l} | \mathbf{e}_{0:T+l-1})$ according to (9), the performance of the model will degrade.

We show a sketch of the resulting *TrAISformer* architecture in Fig. 5.

IV. EXPERIMENTS AND RESULTS

In this section we present our experimental results on a real AIS dataset. We include a benchmarking with respect to state-of-the-art methods for a prediction horizon up to 15 hours. We also report an ablation study to assess the relevance of each component of the proposed model. To facilitate the reproducibility of the work in this paper, we chose a public AIS dataset and made the code of the model available at <https://github.com/CIA-Oceanix/TrAISformer>.

A. Experimental set-up

Dataset: We tested *TrAISformer* on a public AIS dataset provided by the Danish Maritime Authority (DMA)². The dataset comprises AIS observations of cargo and tanker vessels from January 01, 2019 to March 31, 2019. The Region of Interest (ROI) is a rectangle from $(55.5^\circ, 10.3^\circ)$ to $(58.0^\circ, 13.0^\circ)$. The raw dataset (before preprocessing) comprises

²<https://dma.dk/safety-at-sea/navigational-information/download-data>

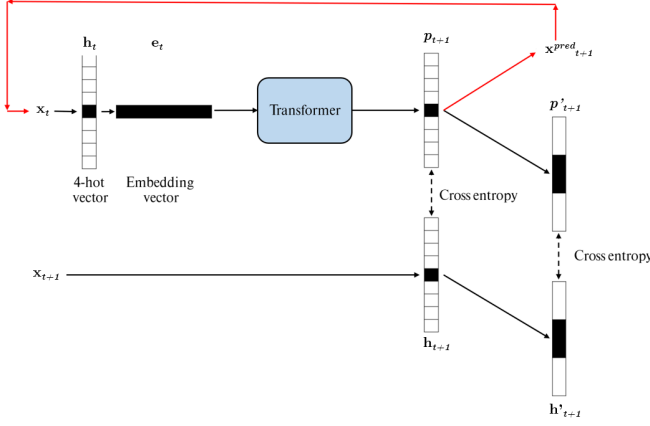


Fig. 5: **Sketch of TrAISformer architecture:** each AIS observation \mathbf{x}_t is discretized into a “four-hot” vector \mathbf{h}_t (for visual purposes, we illustrate an one-hot vector instead of a “four-hot” vector for \mathbf{h}_t), each \mathbf{h}_t is then associated with a high dimensional real-valued embedding vector \mathbf{e}_t . $\mathbf{e}_{0:t}$ will be fed into a transformer network to predict $p_{t+1} \triangleq p(\mathbf{h}_{t+1}|\mathbf{e}_{0:t})$. The training phase minimizes the cross-entropy loss between the true value \mathbf{h}_{t+1} and p_{t+1} . We introduce a “multi-resolution” loss, where the cross-entropy is calculated at different spatial resolutions of \mathbf{h}_{t+1} . In the forecasting phase, we sample vessel position \mathbf{x}_{t+1}^{pred} at time $t+1$ as the “pseudo-inverse” of a four-hot vector \mathbf{h}_{t+1}^{pred} sampled from p_{t+1} . \mathbf{x}_{t+1}^{pred} will be fed back to the network to sample next position (the red path).

$\sim 712\text{M}$ AIS messages. We used AIS data from January 01, 2019 to March 10, 2019 and from March 11, 2019 to March 20, 2019 to train the model and tune the hyper-parameters, respectively. The test set comprises AIS data from March 21, 2019 to March 31, 2019. This dataset was exploited in [16] to evaluate state-of-the-art models for AIS trajectory prediction, including deep learning models.

Data pre-processing: The preprocessing steps are as follows:

- Remove unrealistic speed messages (AIS messages whose $SOG \geq 30$ knots);
- Remove moored or at-anchor vessels;
- Remove AIS observations whose distance to coastline smaller than 1 nautical mile;
- Split non-contiguous voyages into contiguous ones. A contiguous voyage [36], [38] is a voyage whose the maximum interval between two consecutive AIS messages is smaller than a predefined value, here 2 hours;
- Remove AIS voyages whose length is smaller than 20 or those that last less than 4h;
- Remove abnormal messages. An AIS message is considered as abnormal if the empirical speed (calculated by dividing the distance travelled by the corresponding interval between the two consecutive messages) is unrealistic, here above 40 knots;
- Down-sample AIS trajectory data with a sampling rate of 10-minute;
- Split long voyages into shorter ones with a maximum

sequence length of 20 hours.

Hyper-parameters: the results reported in this paper were obtained using a transformer architecture with 8 layers, each layer contains 8 attention heads. The resolution of the “four-hot” vector \mathbf{h}_t was set to 0.01° for lat and lon , 1 knot for SOG and 5° for COG . With this resolution, the corresponding sizes of \mathbf{e}_t^{lat} , \mathbf{e}_t^{lon} , \mathbf{e}_t^{SOG} , \mathbf{e}_t^{COG} for the ROI reported in this paper were 256, 256, 128 and 128, which resulted in a 768-dimensional embedding \mathbf{e}_t . We noticed that when we reduced or increased the resolution of \mathbf{h}_t by 2, the difference in the results was negligible. T was set to 3 hours and L varied from 3 to 17 hours. The model was trained using AdamW optimizer [50] with cyclic cosine decay learning rate scheduler [51]. The learning rate was set to $6e^{-4}$. Other implementation details can be found in the GitHub repository that we shared above. We trained the model on a single GTX 1080 Ti GPU over 50 epochs with early stopping. In terms of computational complexity, it took ~ 60 minutes to process 10 days of data in the test set, which suggests that the model can run in real-time [52].

Benchmarked models: we compare the performance of TrAISformer against different state-of-the-art deep learning models: LSTM seq2seq [12], convolutional seq2seq [53], seq2seq with attention [16], [17], GeoTrackNet [38]. We also include clustering-based methods in our analysis. We notice that it may be difficult to carry out a fair quantitative comparison with clustering-based methods [10], [12], [16], [17], [30], [37]. First, those methods did not state clearly how to address clustering noise and small clusters. Second, most of them use a DBSCAN clustering, which is sensitive to hyper-parameters [10], [17], [30]. Different sets of hyper-parameters could lead to very different results. Third, as mentioned in Section II, clustering-based approaches, such as [17], assume vessels’ trajectories belong to a predefined graph of maritime routes. This assumption does not hold for the considered dataset. This is the reason why [16] restricted their analysis to a subset of the whole dataset. That subset is composed of tankers’ trajectories for a few predefined routes³. Though they only involve a subset of trajectories compared with the other benchmarked approaches, we regard the resulting score in [16] as a score under a best-case scenario for clustering-based methods for the considered ROI.

Evaluation criteria: for each prediction, the prediction error at time step t is calculated as the haversine distance between the true position and the predicted one:

$$d_k = 2R \arcsin \left(\sqrt{\sin^2(\bar{\phi}) + \cos(\phi_1)\cos(\phi_2)\sin^2(\bar{\lambda})} \right), \quad (10)$$

with R the radius of the Earth, $\bar{\phi} \triangleq 0.5(\phi_2 - \phi_1)$, $\bar{\lambda} \triangleq 0.5(\lambda_2 - \lambda_1)$, ϕ_1 and ϕ_2 denote the latitudes, λ_1 and λ_2 denote the longitudes of the predicted position and the true position, respectively.

For probabilistic models, we used a *best-of- N* criterion to evaluate the models, *i.e.* for each model, we sampled N predictions, and reported the best result. In this paper, $N = 16$.

³We may point out that, contrary to the whole dataset, that subset has not been made available.

B. Results

Table I shows the average prediction errors evaluated at 1, 2 and 3-hour-ahead prediction horizons. The ROI contains several waypoints, which makes it highly challenging for a prediction time horizon from 1 hour to 15 hours. At the waypoints, if a model fails to predict the turning direction, its prediction errors will increase significantly, typically above a few nautical miles (nmi) as illustrated for benchmarked models in Table I. *TrAISformer* outperforms all the benchmarked models by a large margin. For instance, for the 2-hour-ahead prediction, it is the only model with an average error below one nautical mile (41% better than the second best model *GeoTracknet*). These results support the ability of *TrAISformer* to capture the multimodal nature of vessels' trajectories, as well as extract useful long-term dependencies to correctly predict vessel paths.

The score of *TrAISformer* is about two times better (0.94 nmi vs. 1.93 nmi) than that of the model proposed in [16], which is one of the current state-of-the-art schemes. We may recall that the performance of this clustering-based scheme refers to a best-case scenario, as it involves only tankers' trajectories for a few maritime routes in the case-study region. We also note that the direct application of state-of-the-art deep learning schemes on the 4-dimensional AIS feature vector, namely LSTM seq2seq [12], convolutional seq2seq [53], seq2seq with attention [16], [17], transformer [39], [48] (see Table. II) leads to poor prediction performances (mean error greater than 6 nmi for a 2-hour-ahead prediction). The second best approach is our previous work *GeoTrackNet* [36], [38]. It shares two key features with *TrAISformer*: i) similar sparse high-dimensional representation of AIS data and ii) probabilistic neural-network-based learning scheme. However, *GeoTrackNet* uses a Variational Recurrent Neural Network (VRNN) [54] instead of a transformer architecture to capture the temporal correlations in data. The better performance of *TrAISformer* over *GeoTrackNet* suggests that transformer may be a better neural architecture for AIS data than VRNN.

To further highlight the importance of the probabilistic feature of *TrAISformer*, we report the score of a deterministic version—denoted as *TrAISformer_No-Stoch*—of *TrAISformer*. Instead of sampling \mathbf{h}_{T+l}^{pred} like in (9), this model outputs the "four-hot" vector with the highest probability, i.e. $\mathbf{h}_{T+l}^{pred} = \text{argmax}_{\mathbf{h}} p(\mathbf{h}_{T+l} | \mathbf{e}_{0:T+l-1})$. The decrease in the prediction performance (from 0.94 to 2.88 for the 2-hour-ahead prediction) provides a clear illustration of the importance of a multimodal representation of vessels' trajectories for the considered case-study. As pointed out previously, two vessels departing from the same port, having the same current position and velocity may go to two different directions at the next waypoint. As a result, the prediction model cannot make correct deterministic forecasts all the time. Models that can predict several possibilities are more relevant. Yet, the deterministic version of *TrAISformer* is still much better than standard seq2seq models, which again stresses the relevance of the transformer architecture as well as of the considered representation of AIS feature vector.

When applying a prediction model to a specific maritime

TABLE I: Mean prediction performance of the benchmarked models (in nautical miles).

Model	1h	2h	3h
LSTM_seq2seq [12]	5.83	8.39	11.64
Conv_seq2seq	4.23	6.77	9.66
LSTM_seq2seq_att	3.35	6.41	9.65
<i>Clustering_LSTM_seq2seq_att</i> ¹ [16]	0.78	1.93	3.66
<i>GeoTrackNet</i> [38]	0.72	1.59	2.67
<i>TrAISformer</i>	0.48	0.94	1.64
<i>TrAISformer_No-Stoch</i>	1.28	2.88	5.02

¹ The result from [1] was evaluated on a subset of the whole dataset, which comprises only tankers trajectories for a predefined number of maritime routes. As such, this is regarded as a best-case scenario.

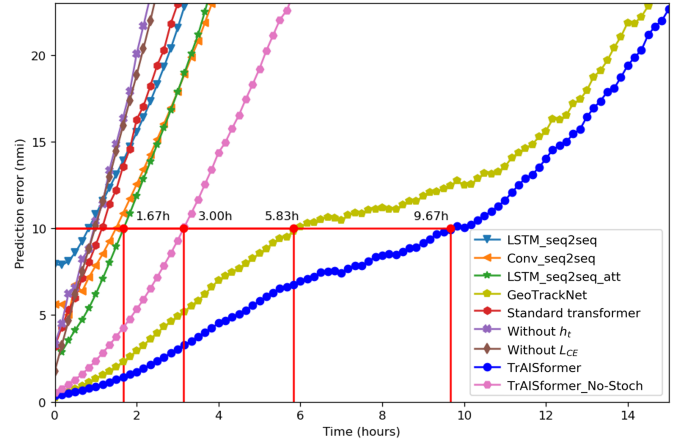


Fig. 6: **Prediction performance w.r.t. prediction time horizon:** we plot for each benchmarked model the mean prediction performance for prediction time horizons from 10 minutes to 15 hours. We also highlight the time horizon up to which the performance of a given model remains below the maximum visibility under good weather conditions (i.e., 10nmi).

downstream task, an important criterion is the maximum meaningful prediction horizon, which is the maximum time horizon where the prediction is still useful. For example, for search and rescue operations, a prediction is helpful if the prediction error is smaller than the visibility. Under clear weather conditions, we may assume a visibility of 10 nmi [55]. Fig. 6 evaluates the prediction horizon of the benchmarked models. In the best case scenario, *TrAISformer* can extend the prediction horizon by a factor of ~ 5.8 compared with current state-of-the-art methods (9.67h for *TrAISformer* vs. 1.67h for LSTM_seq2seq_att).

Fig. 7 depicts prediction examples for *TrAISformer* and the other benchmarked methods. *TrAISformer* successfully samples realistic turning directions to forecast the possible paths followed by the vessels. We recall here that for probabilistic models (*GeoTrackNet*, *TrAISformer*) we report among 16 sampled trajectories the one closest to the real trajectory. We may point out that the model applies not only to the main maritime routes (the first three columns), but also to

less frequent ones (the last column). By contrast, clustering-based methods do not work well in such cases. These four examples show the relatively poor performance of the direct application of sequence-to-sequence deep learning models. *GeoTrackNet* samples realistic trajectories for the first three examples, though not as close to the real ones as the ones predicted by *TrAISformer*. However, it performs poorly for the last one, whereas *TrAISformer* still succeeds in sampling a realistic path.

We further analyse in Fig. 8 the behavior of *TrAISformer* through the activation of an attention block in the first layer of *TrAISformer* for the trajectory shown in Fig. 1. Each row shows the relative importance of each time step in the predicted output. Some remarks raised from this analysis:

- On straight lines, only the information in recent time steps is used to predict the next time step. This aligns with the idea of constant velocity models [56];
- At the waypoints, the model needs to retrieve information from much earlier time steps, especially at the previous waypoints to predict the next time step. For example, row 40 (the red rectangle) depicts the attention weights to compute the prediction at **E**. The model pays more attention to the inputs at **A**, **B**, **C**, **D** and **E**. One intuitive explanation is that the model needs to know where the vessel comes from (points **A**, **B**, **C**), what is the movement pattern of the vessel in the current segment (point **D**), as well as the current position and velocity (point **E**) to guess the movement pattern to come.

As such, this example supports the ability of *TrAISformer* to extract when needed relevant long-term dependencies to predict vessels' trajectories.

C. Ablation study

With a view to assessing the contribution of the different components of *TrAISformer* architecture, we conducted an ablation study:

- First, we removed \mathbf{e}_t and \mathbf{h}_t to show the importance of the high-dimensional encoding. This is equivalent to applying directly a GPT model [48] to 4-dimensional AIS data streams.
- Second, we kept \mathbf{e}_t but removed \mathbf{h}_t to assess the relevance of the sparsity constraint. The embedding $\mathbf{x}_t \rightarrow \mathbf{e}_t$ in this model is a MultiLayer Perceptron (MLP).
- To demonstrate that the classification loss is also critical, we tested a model with the same architecture as *TrAISformer* but using a regression loss as the training loss.

As shown in Tab. II, all the ablated models lead to much worse performance compared with *TrAISformer*. Interestingly, the performance degradation is in the same order of magnitude for the three ablated models, though the impact of the classification-based loss is slightly greater. Overall, these results support the integration of all these components in our architecture to reach the best prediction performance.

V. CONCLUSIONS AND FUTURE WORK

In this paper, we presented a novel model—referred to as *TrAISformer*, for vessel trajectory prediction using AIS data.

The model uses an augmented, sparse and high-dimensional representation of AIS data as well as a state-of-the-art transformer network architecture to learn complex patterns in vessel trajectories. Using a classification-based training loss, *TrAISformer* can capture the multimodal nature of trajectory data. Experiments on real, public AIS data show *TrAISformer* outperforms existing methods by a significant margin. With a 9-hour-ahead prediction error below 10 nmi on a real AIS dataset in a case-study region involving dense and complex maritime traffic patterns, these results open new research avenues for a variety of applications such as search and rescue, port congestion avoidance and maritime surveillance.

Through an ablation study, we have shown that all the above-mentioned components of *TrAISformer* have critical roles in the reported performance. Though transformer architectures are likely not fully explainable [57], [58], we have also shown that the intermediate attention weights of the transformer architecture provides a natural way to explore how *TrAISformer* exploits the past AIS data to compute its predictions of the future trajectory. This supports that the learned transformer representation could be of interest beyond the considered application to prediction tasks.

Future work could further improve the architecture and develop the applications of *TrAISformer* framework. Among others, we may cite the learning of conditional *TrAISformer* w.r.t. weather conditions as the latter clearly impact vessels' movement. The combination of *TrAISformer* with other learning-based modules for classification and anomaly detections [38] is also of interest. Recent advances in the exploitation of AIS data for the inversion of sea surface parameters [59], [60] may also be an appealing line of research for our future work.

REFERENCES

- [1] Z. Ou and J. Zhu, "AIS Database Powered by GIS Technology for Maritime Safety and Security," *The Journal of Navigation*, vol. 61, no. 4, pp. 655–665, Oct. 2008, publisher: Cambridge University Press.
- [2] I. Varlamis, K. Tserpes, and C. Sardanios, "Detecting Search and Rescue Missions from AIS Data," in *2018 IEEE 34th International Conference on Data Engineering Workshops (ICDEW)*, Apr. 2018, pp. 60–65, iSSN: 2473-3490.
- [3] T. Fabbri, R. Vicen-Bueno, R. Grasso, G. Pallotta, L. M. Millefiori, and L. Cazzanti, "Optimization of surveillance vessel network planning in maritime command and control systems by fusing METOC & AIS vessel traffic information," in *OCEANS 2015 - Genova*, May 2015, pp. 1–7.
- [4] E. Tu, G. Zhang, L. Rachmawati, E. Rajabally, and G.-B. Huang, "Exploiting AIS Data for Intelligent Maritime Navigation: A Comprehensive Survey," *IEEE Transactions on Intelligent Transportation Systems*, 2017.
- [5] J. M. Mou, C. v. d. Tak, and H. Ligteringen, "Study on collision avoidance in busy waterways by using AIS data," *Ocean Engineering*, vol. 37, no. 5, pp. 483–490, Apr. 2010.
- [6] C. Liu, J. Liu, X. Zhou, Z. Zhao, C. Wan, and Z. Liu, "AIS data-driven approach to estimate navigable capacity of busy waterways focusing on ships entering and leaving port," *Ocean Engineering*, vol. 218, p. 108215, Dec. 2020.
- [7] M. J. Kang, S. Zohoori, M. Hamidi, and X. Wu, "Study of narrow waterways congestion based on automatic identification system (AIS) data: A case study of Houston Ship Channel," *Journal of Ocean Engineering and Science*, Oct. 2021.
- [8] G. Soldi, D. Gaglione, N. Forti, A. Di Simone, F. C. Daffin, G. Bottini, D. Quattrociochi, L. M. Millefiori, P. Braca, S. Carniel, P. Willett, A. Iodice, D. Riccio, and A. Farina, "Space-based Global Maritime Surveillance. Part II: Artificial Intelligence and Data Fusion Techniques," *IEEE Aerospace and Electronic Systems Magazine*, vol. 36, no. 9, pp. 30–42, Sep. 2021, arXiv:2011.11338 [eess].

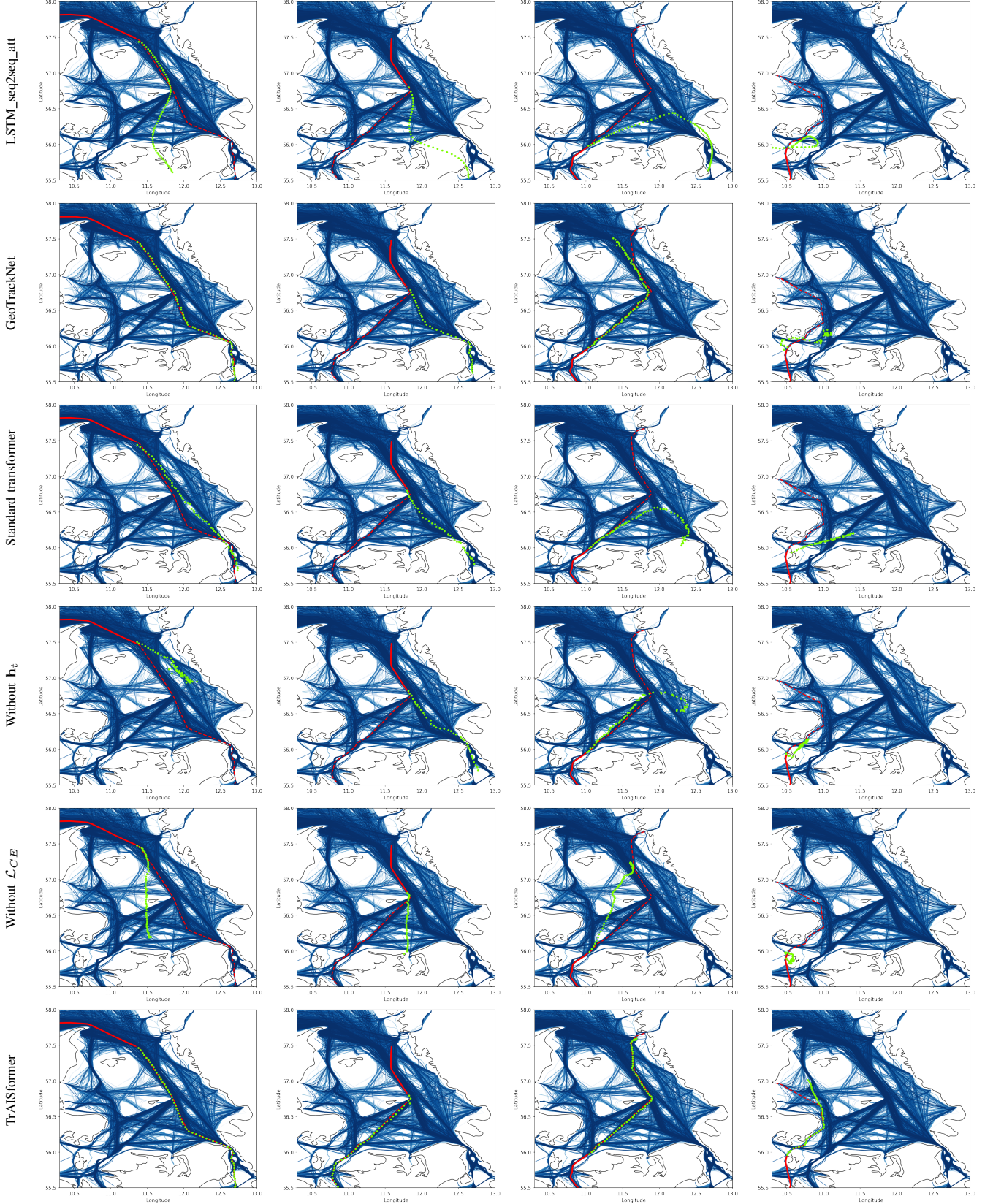


Fig. 7: Examples of AIS trajectory predictions: each column depicts the predictions of a given real AIS trajectory. The rows refer to the benchmarked models. For each example, we display the AIS observations $\mathbf{x}_{0:T}$ used as the input by all models —, the real AIS trajectory —, and the predicted trajectory —.

TABLE II: Mean prediction performance (in nautical miles) of the models in the ablation study.

Model	AIS data representation	Embedding $\mathbf{x}_t \rightarrow \mathbf{e}_k$	Loss function	1h	2h	3h
Without \mathbf{e}_t and \mathbf{h}_t (standard transformer)	$[\text{lat}, \text{lon}, \text{SOG}, \text{COG}]^T$	None	\mathcal{L}_{MSE}	4.75	8.36	11.40
Without \mathbf{h}_t	$[\text{lat}, \text{lon}, \text{SOG}, \text{COG}]^T \rightarrow \mathbf{e}_t$	MLP	\mathcal{L}_{MSE}	5.02	9.69	15.04
Without the classification loss \mathcal{L}_{CE}	“four-hot” vector $\rightarrow \mathbf{e}_t$	Via \mathbf{h}_t	\mathcal{L}_{MSE}	5.53	10.64	16.06
<i>TrAISformer</i>	“four-hot” vector $\rightarrow \mathbf{e}_t$	Via \mathbf{h}_t	\mathcal{L}_{CE}	0.48	0.94	1.64

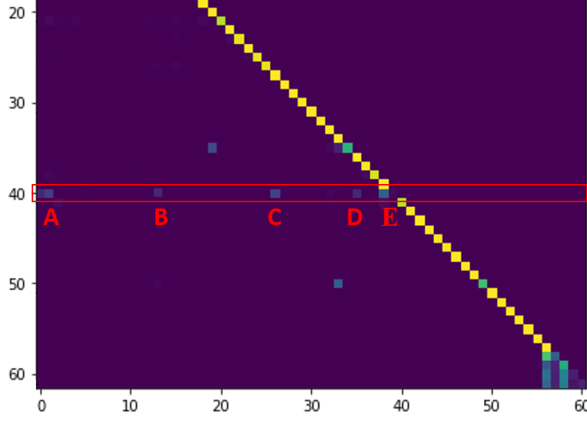


Fig. 8: Visualization of the activation of one attention block of *TrAISformer* for the trajectory shown in Fig. 1. Horizontal axis: input time step; vertical axis: output time step. Each row shows which parts of the input that the model pays attention to in order to compute the output at the corresponding time step.

[9] B. Ristic, B. La Scala, M. Morelande, and N. Gordon, “Statistical analysis of motion patterns in AIS Data: Anomaly detection and motion prediction,” in *2008 11th International Conference on Information Fusion*, Jun. 2008, pp. 1–7.

[10] F. Mazzarella, V. F. Arguedas, and M. Vespe, “Knowledge-based vessel position prediction using historical AIS data,” in *2015 Sensor Data Fusion: Trends, Solutions, Applications (SDF)*, Oct. 2015, pp. 1–6.

[11] H. Rong, A. P. Teixeira, and C. Guedes Soares, “Ship trajectory uncertainty prediction based on a Gaussian Process model,” *Ocean Engineering*, vol. 182, pp. 499–511, Jun. 2019.

[12] N. Forti, L. M. Millefiori, P. Braca, and P. Willett, “Prediction of Vessel Trajectories From AIS Data Via Sequence-To-Sequence Recurrent Neural Networks,” in *ICASSP 2020 - 2020 IEEE International Conference on Acoustics, Speech and Signal Processing (ICASSP)*, May 2020, pp. 8936–8940, iSSN: 2379-190X.

[13] T. A. Volkova, Y. E. Balykina, and A. Bepalov, “Predicting ship trajectory based on neural networks using AIS data,” *Journal of Marine Science and Engineering*, vol. 9, no. 3, p. 254, 2021, iSSN: 2077-1312 Publisher: MDPI.

[14] B. Murray and L. P. Perera, “Ship behavior prediction via trajectory extraction-based clustering for maritime situation awareness,” *Journal of Ocean Engineering and Science*, Mar. 2021.

[15] J. Park, J. Jeong, and Y. Park, “Ship trajectory prediction based on bi-LSTM using spectral-clustered AIS data,” *Journal of Marine Science and Engineering*, vol. 9, no. 9, p. 1037, 2021, iSSN: 2077-1312 Publisher: MDPI.

[16] S. Capobianco, L. M. Millefiori, N. Forti, P. Braca, and P. Willett, “Deep Learning Methods for Vessel Trajectory Prediction based on Recurrent Neural Networks,” *IEEE Transactions on Aerospace and Electronic Systems*, pp. 1–1, 2021, conference Name: IEEE Transactions on Aerospace and Electronic Systems.

[17] B. Murray and L. P. Perera, “An AIS-based deep learning framework for regional ship behavior prediction,” *Reliability Engineering & System Safety*, p. 107819, May 2021.

[18] L. M. Millefiori, G. Pallotta, P. Braca, S. Horn, and K. Bryan, “Validation

of the Ornstein-Uhlenbeck route propagation model in the Mediterranean Sea,” in *OCEANS 2015 - Genova*, May 2015, pp. 1–6.

[19] L. M. Millefiori, P. Braca, K. Bryan, and P. Willett, “Modeling vessel kinematics using a stochastic mean-reverting process for long-term prediction,” *IEEE Transactions on Aerospace and Electronic Systems*, vol. 52, no. 5, pp. 2313–2330, Oct. 2016.

[20] A. Rudenko, L. Palmieri, M. Herman, K. M. Kitani, D. M. Gavrila, and K. O. Arras, “Human motion trajectory prediction: a survey,” *The International Journal of Robotics Research*, vol. 39, no. 8, pp. 895–935, Jul. 2020, publisher: SAGE Publications Ltd STM.

[21] F. Leon and M. Gavrilescu, “A Review of Tracking and Trajectory Prediction Methods for Autonomous Driving,” *Mathematics*, vol. 9, no. 6, p. 660, Jan. 2021, number: 6 Publisher: Multidisciplinary Digital Publishing Institute.

[22] A. Gupta, J. Johnson, L. Fei-Fei, S. Savarese, and A. Alahi, “Social GAN: Socially Acceptable Trajectories With Generative Adversarial Networks,” 2018, pp. 2255–2264.

[23] A. Vemula, K. Muelling, and J. Oh, “Social Attention: Modeling Attention in Human Crowds,” in *2018 IEEE International Conference on Robotics and Automation (ICRA)*, May 2018, pp. 4601–4607, iSSN: 2577-087X.

[24] A. Sadeghian, V. Kosaraju, A. Sadeghian, N. Hirose, H. Rezatofighi, and S. Savarese, “SoPhie: An Attentive GAN for Predicting Paths Compliant to Social and Physical Constraints,” 2019, pp. 1349–1358.

[25] T. Zhao, Y. Xu, M. Monfort, W. Choi, C. Baker, Y. Zhao, Y. Wang, and Y. N. Wu, “Multi-Agent Tensor Fusion for Contextual Trajectory Prediction,” 2019, pp. 12 126–12 134.

[26] T. Salzmann, B. Ivanovic, P. Chakravarty, and M. Pavone, “Trajectron++: Dynamically-Feasible Trajectory Forecasting With Heterogeneous Data,” *arXiv:2001.03093 [cs]*, Jan. 2021, arXiv: 2001.03093.

[27] P. Coscia, P. Braca, L. M. Millefiori, F. A. N. Palmieri, and P. Willett, “Multiple Ornstein-Uhlenbeck Processes for Maritime Traffic Graph Representation,” *IEEE Transactions on Aerospace and Electronic Systems*, pp. 1–1, 2018.

[28] I. Varlamis, K. Tserpes, M. Etemad, A. S. JÄ^nior, and S. Matwin, “A Network Abstraction of Multi-vessel Trajectory Data for Detecting Anomalies,” in *EDBT/ICDT Workshops*, 2019.

[29] R. Bosnjak, L. Simunovic, and Z. Kavran, “Automatic identification system in maritime traffic and error analysis,” *Transactions on maritime science*, vol. 1, no. 02, pp. 77–84, 2012, iSSN: 1848-3305 Publisher: Pomorski fakultet u Splitu.

[30] Y. Suo, W. Chen, C. Claramunt, and S. Yang, “A Ship Trajectory Prediction Framework Based on a Recurrent Neural Network,” *Sensors*, vol. 20, no. 18, p. 5133, Jan. 2020, number: 18 Publisher: Multidisciplinary Digital Publishing Institute.

[31] L. P. Perera, P. Oliveira, and C. G. Soares, “Maritime Traffic Monitoring Based on Vessel Detection, Tracking, State Estimation, and Trajectory Prediction,” *IEEE Transactions on Intelligent Transportation Systems*, vol. 13, no. 3, pp. 1188–1200, Sep. 2012.

[32] S. Fossen and T. I. Fossen, “Extended Kalman Filter Design and Motion Prediction of Ships Using Live Automatic Identification System (AIS) Data,” in *2018 2nd European Conference on Electrical Engineering and Computer Science (EECS)*, Dec. 2018, pp. 464–470.

[33] C. Wang, H. Ren, and H. Li, “Vessel trajectory prediction based on AIS data and bidirectional GRU,” in *2020 International Conference on Computer Vision, Image and Deep Learning (CVIDL)*, Jul. 2020, pp. 260–264.

[34] W. Li, C. Zhang, J. Ma, and C. Jia, “Long-term Vessel Motion Prediction by Modeling Trajectory Patterns with AIS Data,” in *2019 5th International Conference on Transportation Information and Safety (ICTIS)*, Jul. 2019, pp. 1389–1394.

[35] H. Tang, Y. Yin, and H. Shen, “A model for vessel trajectory prediction based on long short-term memory neural network,” *Journal of Marine Engineering & Technology*, vol. 0,

no. 0, pp. 1–10, Sep. 2019, publisher: Taylor & Francis _eprint: <https://doi.org/10.1080/20464177.2019.1665258>.

- [36] D. Nguyen, R. Vadaine, G. Hajdich, R. Garelo, and R. Fablet, “A Multi-task Deep Learning Architecture for Maritime Surveillance using AIS Data Streams,” in *2018 IEEE International Conference on Data Science and Advanced Analytics (DSAA)*, Oct. 2018.
- [37] G. Pallotta, M. Vespe, and K. Bryan, “Vessel Pattern Knowledge Discovery from AIS Data: A Framework for Anomaly Detection and Route Prediction,” *Entropy*, vol. 15, no. 6, pp. 2218–2245, Jun. 2013.
- [38] D. Nguyen, R. Vadaine, G. Hajdich, R. Garelo, and R. Fablet, “GeoTrackNet-A Maritime Anomaly Detector using Probabilistic Neural Network Representation of AIS Tracks and A Contrario Detection,” *IEEE Transactions on Intelligent Transportation Systems*, Feb. 2021.
- [39] A. Vaswani, N. Shazeer, N. Parmar, J. Uszkoreit, L. Jones, A. N. Gomez, A. Kaiser, and I. Polosukhin, “Attention is All you Need,” in *Advances in Neural Information Processing Systems*, vol. 30. Curran Associates, Inc., 2017.
- [40] Y. LeCun, Y. Bengio, and G. Hinton, “Deep learning,” *Nature*, vol. 521, no. 7553, pp. 436–444, May 2015.
- [41] I. Goodfellow, Y. Bengio, and A. Courville, *Deep learning*. MIT press, 2016.
- [42] D. P. Kingma and M. Welling, “Auto-Encoding Variational Bayes,” *arXiv:1312.6114 [cs, stat]*, Dec. 2013, arXiv: 1312.6114.
- [43] D. J. Rezende and S. Mohamed, “Variational inference with normalizing flows,” *arXiv preprint arXiv:1505.05770*, 2015.
- [44] Y. Pu, Z. Gan, R. Henao, X. Yuan, C. Li, A. Stevens, and L. Carin, “Variational Autoencoder for Deep Learning of Images, Labels and Captions,” in *Advances in Neural Information Processing Systems 29*, D. D. Lee, M. Sugiyama, U. V. Luxburg, I. Guyon, and R. Garnett, Eds. Curran Associates, Inc., 2016, pp. 2352–2360.
- [45] A. Vahdat and J. Kautz, “NVAE: A Deep Hierarchical Variational Autoencoder,” in *Advances in Neural Information Processing Systems*, vol. 33. Curran Associates, Inc., 2020, pp. 19667–19679.
- [46] A. Ng, “Sparse autoencoder,” *CS294A Lecture notes*, vol. 72, no. 2011, pp. 1–19, 2011.
- [47] P. Dijt and P. Mettes, “Trajectory Prediction Network for Future Anticipation of Ships,” in *Proceedings of the 2020 International Conference on Multimedia Retrieval*, ser. ICMR ’20. New York, NY, USA: Association for Computing Machinery, Jun. 2020, pp. 73–81.
- [48] A. Radford, K. Narasimhan, T. Salimans, and I. Sutskever, “Improving Language Understanding by Generative Pre-Training,” p. 12, 2018.
- [49] M. Phuong and M. Hutter, “Formal Algorithms for Transformers,” *arXiv preprint arXiv:2207.09238*, 2022.
- [50] I. Loshchilov and F. Hutter, “Decoupled Weight Decay Regularization,” *arXiv:1711.05101 [cs, math]*, Jan. 2019, arXiv: 1711.05101.
- [51] —, “SGDR: Stochastic Gradient Descent with Warm Restarts,” *arXiv:1608.03983 [cs, math]*, May 2017, arXiv: 1608.03983.
- [52] D. Nguyen, M. Simonin, G. Hajdich, R. Vadaine, C. Tedeschi, and R. Fablet, “Detection of Abnormal Vessel Behaviors from AIS data using GeoTrackNet: from the Laboratory to the Ocean,” in *21st IEEE International Conference on Mobile Data Management (MDM)*, 2020.
- [53] J. Gehring, M. Auli, D. Grangier, D. Yarats, and Y. N. Dauphin, “Convolutional Sequence to Sequence Learning,” in *International Conference on Machine Learning*. PMLR, Jul. 2017, pp. 1243–1252, iSSN: 2640-3498.
- [54] J. Chung, K. Kastner, L. Dinh, K. Goel, A. Courville, and Y. Bengio, “A Recurrent Latent Variable Model for Sequential Data,” in *Advances in neural information processing systems*, Jun. 2015, pp. 2980–2988.
- [55] C. A. Blance, *Norie’s Nautical Tables*. Imray, Laurie, Norie and Wilson Ltd, 2019.
- [56] Z. Xiao, X. Fu, L. Zhang, and R. S. M. Goh, “Traffic Pattern Mining and Forecasting Technologies in Maritime Traffic Service Networks: A Comprehensive Survey,” *IEEE Transactions on Intelligent Transportation Systems*, vol. 21, no. 5, pp. 1796–1825, May 2020, conference Name: IEEE Transactions on Intelligent Transportation Systems.
- [57] A. Adadi and M. Berrada, “Peeking Inside the Black-Box: A Survey on Explainable Artificial Intelligence (XAI),” *IEEE Access*, vol. 6, pp. 52 138–52 160, 2018, conference Name: IEEE Access.
- [58] A. Barredo Arrieta, N. D’Áaz-Rodríguez, J. Del Ser, A. Bannetot, S. Tabik, A. Barbado, S. Garcia, S. Gil-Lopez, D. Molina, R. Benjamins, R. Chatila, and F. Herrera, “Explainable Artificial Intelligence (XAI): Concepts, taxonomies, opportunities and challenges toward responsible AI,” *Information Fusion*, vol. 58, pp. 82–115, Jun. 2020.
- [59] S. Benaichouche, C. Le Goff, Y. Guichoux, F. Rousseau, and R. Fablet, “Unsupervised Reconstruction of Sea Surface Currents from AIS Maritime Traffic Data Using Learnable Variational Models,” in *ICASSP 2021*

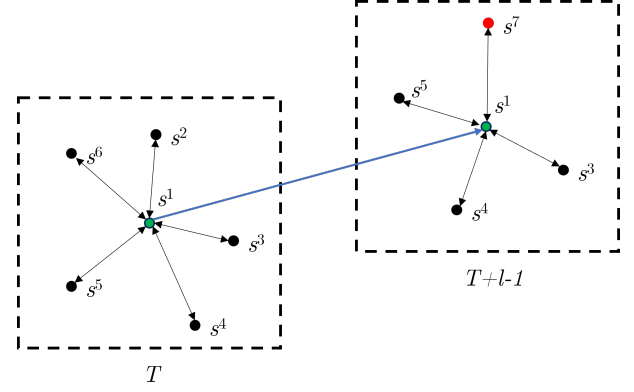


Fig. 9: Demonstration of the intractability of the modeling of the interactions between agents in long-term trajectory prediction. Suppose that we want to predict the trajectory at a long-term horizon of agent s^1 (green dot). At time T , there are 6 other agents (s^2, \dots, s^6) in the vicinity (dashed rectangle). Their interactions with s^1 are illustrated by the double-headed arrows. At time $T+l-1$ in the long future, s^2 and s^6 would have departed from s^1 ; and a new, unknown agent s^7 (red dot) would appear near s^1 . The new vicinity of s^1 would be unknown to the model. Hence, the modeling of the interactions between agents become intractable.

- 2021 IEEE International Conference on Acoustics, Speech and Signal Processing (ICASSP), Jun. 2021, pp. 4100–4104, iSSN: 2379-190X.

- [60] S. Benaichouche, C. Legoff, Y. Guichoux, F. Rousseau, and R. Fablet, “Unsupervised Reconstruction of Sea Surface Currents from AIS Maritime Traffic Data Using Trainable Variational Models,” *Remote Sensing*, vol. 13, no. 16, p. 3162, Jan. 2021, number: 16 Publisher: Multidisciplinary Digital Publishing Institute.
- [61] B. Ivanovic and M. Pavone, “The Trajectron: Probabilistic Multi-Agent Trajectory Modeling With Dynamic Spatiotemporal Graphs,” in *2019 IEEE/CVF International Conference on Computer Vision (ICCV)*. Seoul, Korea (South): IEEE, Oct. 2019, pp. 2375–2384.

APPENDIX

A. Why pedestrian and vehicle trajectory prediction models do not apply to long-term AIS trajectory prediction

In this appendix we provide the mathematical demonstration of why pedestrian and vehicle trajectory prediction models do not apply to long-term AIS trajectory prediction.

Let us denote $\mathbf{x}_t^{s^i}$ an observation of an agent s^i at time t . For example, for pedestrian and vehicle trajectory prediction, s^i is either a pedestrian or a vehicle, and $\mathbf{x}_t^{s^i}$ is its position on the map; for AIS trajectory prediction, s^i is a vessel, and $\mathbf{x}_t^{s^i}$ is its AIS message. The trajectory of agent s^i from t_1 to t_2 ($t_2 > t_1$) is then represented by a sequence of observations $\mathbf{x}_{t_1:t_2}^{s^i} = \{\mathbf{x}_{t_1}^{s^i}, \mathbf{x}_{t_1+1}^{s^i}, \dots, \mathbf{x}_{t_2}^{s^i}\}$. At time t , the group of other agents in the vicinity of s^i is denoted as \mathbf{V}_t^i , and their historical trajectories are denoted as $\mathbf{x}_{0:t}^{\mathbf{V}_t^i}$.

With those notations, trajectory prediction in the context of this paper means to forecast the trajectory of an agent s^i L timesteps ahead, given the historical observations until T of this agent and the others in the vicinity, by maximizing the likelihood:

$$p(\mathbf{x}_{T+1:T+L}^{s^i} | \mathbf{x}_{0:T}^{s^i}, \mathbf{x}_{0:T}^{\mathbf{V}_T^i}). \quad (11)$$

Here we use p in the broad sense, which includes deterministic models.

The $\mathbf{x}_{0:T}^{s^i}$ part in the conditioning side of (11) embeds the intention of the agent, while the $\mathbf{x}_{0:T}^{\mathbf{V}_T^i}$ part embeds the interactions with the environment. State-of-the-art methods for pedestrian and vehicle trajectory prediction focus on how to model and incorporate these two terms. Among them we may cite S-LSTM [22], S-GAN [22], S-ATTN [23], SoPhie [24], MATF [25], Trajection

[61], Trajectron++ [26], etc. Those models use deep neural networks such as LSTM or GAN (Generative Adversarial Network) to capture correlations in historical data, and some pooling techniques to embed the interactions between agents. Although those methods have shown promising results on the corresponding datasets, they are not suitable for long-term vessel trajectory prediction. First, the prediction horizons considered in those works are from a few seconds to a few minutes, which are too short for maritime applications. Second, those works address a different type of maneuvers, of which the movement of an agent depends highly on the interactions with other agents and the surrounding environment. For maritime traffic contexts, and at a medium/long time horizon, the path that a vessel will make depends mainly on where it wants to go to, and is barely effected by the interactions with other vessels in the vicinity at the current moment. Mathematically, this means at time T we have the approximation:

$$p(\mathbf{x}_{T+l}^{s^i} | \mathbf{x}_{0:T}^{s^i}, \mathbf{V}_{0:T}^{s^i}) \approx p(\mathbf{x}_{T+l}^{s^i} | \mathbf{x}_{0:T}^{s^i}) \Big|_{l > 1}. \quad (12)$$

One may argue that we could use the predicted value of $\mathbf{x}_{0:T+l-1}^{s^i}$ and $\mathbf{x}_{0:T+l-1}^{s^i}$ to estimate $\mathbf{x}_{T+l}^{s^i}$. However, in order to predict $\mathbf{x}_{0:T+l-1}^{s^i}$, we need to predict the trajectory of all the agents in the vicinity of s^i at $T+l-1$. This is an expensive or even intractable approach. For example, an unknown agent may join the ROI (see Fig. 9).

Those above may explain why none of the mentioned methods has been explored in maritime contexts.

Note that if we remove $\mathbf{V}_{0:T}^{s^i}$ from (11), this objective function becomes (1), which is the objective function used in AIS trajectory prediction. Likewise, if we remove the parts that encode the interactions between agents in some of the pedestrian and vehicle trajectory prediction models mentioned above, we get models that have similar architectures with those designed for AIS trajectory prediction. For example, if we remove the interactions between agents part in Trajectron [61], it becomes an LSTM_seq2seq model.